



Building thiol and metal-thiolate functions into coordination nets: Clues from a simple molecule

Jun He^a, Chen Yang^a, Zhengtao Xu^{a,*}, Matthias Zeller^b, Allen D. Hunter^b, Jianhua Lin^c

^a Department of Biology and Chemistry, City University of Hong Kong, 83 Tat Chee Avenue, Kowloon, Hong Kong, China

^b Department of Chemistry, Youngstown State University, One University Plaza, Youngstown, OH 44555, USA

^c Beijing National Laboratory for Molecular Sciences, State Key Laboratory of Rare Earth Materials Chemistry and Applications, College of Chemistry and Molecular Engineering, Peking University, Beijing 100871, China

ARTICLE INFO

Article history:

Received 24 January 2009

Received in revised form

13 April 2009

Accepted 18 April 2009

Available online 3 May 2009

Keywords:

Metal-thiolate networks

Coordination networks

Bifunctional ligands

Crystal engineering

ABSTRACT

The simple and easy-to-prepare bifunctional molecule 2,5-dimercapto-1,4-benzenedicarboxylic acid (H₄DMBD) interacts with the increasingly harder metal ions of Cu⁺, Pb²⁺ and Eu³⁺ to form the coordination networks of Cu₆(DMBD)₃(en)₄(Hen)₆ (**1**), Pb₂(DMBD)(en)₂ (**2**) and Eu₂(H₂DMBD)₃(DEF)₄ (**3**), where the carboxyl and thiol groups bind with distinct preference to the hard and soft metal ions, respectively. Notably, **1** features uncoordinated carboxylate groups and Cu₃ cluster units integrated via the thiolate groups into an extended network with significant interaction between the metal centers and the organic molecules; **2** features a 2D coordination net based on the mercapto and carboxylic groups all bonded to the Pb²⁺ ions; **3** features free-standing thiol groups inside the channels of a metal-carboxylate-based network. This study illustrates the rich solid state structural features and potential functions offered by the carboxyl-thiol combination.

© 2009 Elsevier Inc. All rights reserved.

1. Introduction

In the fast-growing field of crystal engineering of molecular-based networks (e.g., hydrogen-bonded networks and coordination networks/metal-organic frameworks) [1], it is of interest to develop ligand or ligand systems that unveil new design strategies for network construction or lead to enhanced properties of the solids. Among these, multitopic carboxylic acids (such as 1,4-benzenedicarboxylic and 1,3,5-benzenetricarboxylic acids) have been widely used to construct metal-organic frameworks (MOFs) that sustain substantial porous features [2]. One significant factor that facilitates the crystallization process here might be that the chemically hard carboxylate unit bonds to metal centers (especially labile ones such as Zn²⁺ and Cu²⁺) with distinct ionic character. The ionicity provides for effective solvation of the ions in polar solvents, and might promote the reversibility of the carboxylate–metal bond formation (e.g., under hydrothermal conditions). On the other hand, the metal–carboxylate frameworks generally feature weak electronic interaction between the metal centers and the organic π -system, which might, in part, also be due to the strong ionic character of the metal–carboxylate interaction. The thiol function (–SH), by comparison, presents a markedly different situation. It is a much softer donor, and bonds

to metal centers with more covalent features—the bonding strength is often strong, and affords much less reversibility. In general, solid state compounds of metal sulfides and thiolates feature significant electronic properties (e.g., electrical conductivity), and are of great interest as electronic materials [3]. The crystallization of solid state networks based on the metal–thiolate linkage is, however, difficult largely due to the irreversible bond formation process (even though significant progresses are being made in this direction regarding thiolate [4] and thiocarboxylate [5] systems).

In this paper, we draw on the molecule 2,5-dimercapto-1,4-benzenedicarboxylic acid (H₄DMBD, chart 1, synthesis known [6]) as a bifunctional building block in order to explore the potential synergism between the carboxylic and thiol functions. First, the carboxylic acid groups might provide better solubility either by reducing the electron density of the thiol groups and weaken its interaction with metal ions, or by forming an ionic solvated species in an alkaline solvent (e.g., ethylenediamine). Second, by using hard metal ions such as Zn(II) and RE(III) (RE: rare earth elements), one might selectively engage the carboxylic groups while leaving –SH groups as free-standing units in the resultant networks, and thus create opportunities for post-crystallization (post-synthetic) modifications [7] and other applications. This work thus differs significantly from our recent work on systems containing carboxylic and thioether functions [8] in two regards: (1) unlike the weak and reversible thioether coordination bonds (which largely favor the crystallization of thioether–metal

* Corresponding author. Fax: +852 2788 7406.

E-mail address: zhengtao@cityu.edu.hk (Z. Xu).

coordination nets [9]), thiolate–metal bonds are much stronger and tend to generate more significant electronic interaction with the metal centers; (2) the thiol group is more reactive than the thioether group, and can potentially react with a wider range of reagents (as a free-standing group) in the post-crystallization modification.

Presented here are a number of networks based on H₄DMBD and the ions of Cu⁺, Pb²⁺ and Eu³⁺ with varying chemical hardness η_A values of 6.3, 8.5 and 15.4, respectively [10]. Together these networks exhibit the salient features of simultaneous bonding of the carboxyl and thiol groups to metal centers and extensive decoration of a channel structure with free-standing thiol groups—features that have been little explored in coordination networks and could open new possibilities for functionalizing these solid state materials.

2. Experimental section

General Procedure: Starting materials, reagents and solvents were purchased from commercial sources (Aldrich and Acros) and used without further purification. Elemental analysis was performed with a Vario EL III CHN elemental analyzer. FT-IR spectra were measured using a Nicolet Avatar 360 FT-IR spectrophotometer. X-ray powder diffraction patterns of **1**, **2** and **3** for the bulk samples (the powder samples were spread onto glass slides for data collection) were collected at room temperature on a Siemens D500 powder diffractometer (CuK α , $\lambda = 1.5418 \text{ \AA}$). The power of the sealed X-ray tube was 40 kV and 30 mA. The program Mercury was used in the calculation of powder patterns from single crystal structures. Optical diffuse reflectance measurements were performed at room temperature with a PerkinElmer Lambda 750 spectrophotometer. The solid sample was finely ground and pressed between two Mylar tapes (sample thickness is about 1.0 mm and much greater than the particle size, and therefore an ideal diffuse reflection can be assumed). The sample was held against a white background for data collection.

2.1. Syntheses

2.1.1. Crystallization of **1**

H₄DMBD (2.3 mg, 10.0 μmol) and Cu(OAc)₂·H₂O (4.0 mg, 20.0 μmol) were loaded into a heavy-wall glass tube, and en (1,2-ethylenediamine, 0.8 ml, anhydrous) was added. The tube was then sealed and heated at 100 °C in a programmable oven for 48 h, followed by slow cooling (0.1 °C/min) to rt, during which yellow block-like single crystals suitable for single crystal X-ray diffraction were formed (3.8 mg, 60% yield based on H₄DMBD). Chemical analysis of the product C₂₂H₄₆Cu₃N₁₀O₆S₃ yields the following: Calcd [C (31.70%), H (5.56%) and N (16.80%)]; found [C (32.06%), H (5.73%) and N (16.50%)]. IR (ν/cm^{-1}): 3308s, 3224s, 2945s, 2883s, 2129w, 1718w, 1673s, 1633s, 1581s, 1550s, 1457s, 1375s, 1308s, 1145w, 1080s, 1044s, 1019w, 984w, 828s and 715w. Compound **1** could also be obtained by using CuCl as the Cu source under similar reaction conditions as above, albeit with **1** formed as much smaller crystallites and in lower yields.

2.1.2. Crystallization of **2**

H₄DMBD (2.3 mg, 10.0 μmol) and PbCl₂ (8.4 mg, 30.0 μmol) were loaded into a heavy-wall glass tube, and en (0.8 ml, anhydrous) was added. The tube was then sealed and heated at 100 °C in a programmable oven for 48 h, followed by slow cooling (0.1 °C/min) to rt, during which colorless block-like single crystals suitable for single crystal X-ray diffraction were formed (6.0 mg, 80% yield based on H₄DMBD). Incidentally, the product of **2** can

also be prepared from Pb(OAc)₂·H₂O instead of PbCl₂, albeit in a lower yield. Chemical analysis of the product C₁₂H₁₈N₄O₄Pb₂S₂ yields the following: Calcd [C (18.94%), H (2.38%) and N (7.36%)]; found [C (18.79%), H (2.56%) and N (7.62%)]. IR (ν/cm^{-1}): 3422w, 3350w, 2914s, 1700w, 1684s, 1647s, 1559s, 1541s, 1497s, 1458w, 1383s, 1303w, 1250w, 1082w, 1021w, 837s, 790w and 653w.

2.1.3. Crystallization of **3**

H₄DMBD (4.6 mg, 20.0 μmol) and EuCl₃·6H₂O (14.8 mg, 40.0 μmol) were loaded into a heavy-wall glass tube, and *N,N*-diethylformamide (DEF) (1.0 ml, anhydrous) was then added. The tube was then sealed and heated at 100 °C in a programmable oven for 48 h, followed by slow cooling down (0.1 °C/min) to rt, during which yellow rod-like single crystals suitable for single crystal X-ray diffraction were formed (5.9 mg, 65% yield based on H₄DMBD). Chemical analysis of the product C₂₂H₂₈EuN₂O₈S₃ yields the following: Calcd [C (37.93%), H (4.05%) and N (4.02%)]; found [C (38.03%), H (4.23%) and N (3.94%)]. IR (ν/cm^{-1}): 3421w, 2978s, 2937s, 2522w, 1704w, 1653s, 1636s, 1599s, 1558s, 1506w, 1458s, 1395s, 1268s, 1212s, 1123w, 1102s, 947w, 895w, 853s, 844s, 823s, 801s and 655s.

2.2. Crystallography

X-ray datasets of the single crystal samples were collected on a Bruker AXS SMART APEX CCD system using MoK α ($\lambda = 0.71073 \text{ \AA}$) radiation at 100(2)K. The structures were solved and refined by full-matrix least-squares on F_o^2 using SHELXL 6.14. In the copper complex (**1**) one amine moiety of one ethylenediamine unit and one whole ethylenediamine molecule located on an inversion center and are disordered over two positions with a common occupancy ratio of 0.672(5) to 0.368(5). The ADPs of the atoms of the minor disordered molecule were set to be identical to those of the major one and the C–C distance across the inversion center of the minor occupied unit was set to be 1.50(2) Å. Hydrogen atoms for all but the disordered amine and ammonium atoms were localized in difference density Fourier maps. Eventually all but the amine H atoms were placed in calculated positions with standard X–H bond lengths and angles. Amine H atoms were placed based on Fourier maps for non-disordered moieties and in sensible positions based on hydrogen bonding considerations for disordered units. All amine N–H atoms were restrained to be the same within a standard deviation of 0.02 Å and for the disordered units the C···H distances were also restrained to be each the same. H···H distances for H10a/H10b and H10c/H10d were restrained to be 1.44(2) Å. In the europium complex (**3**) one of the coordinated diethyl formamide ligands is disordered over two positions by inversion of the ethyl moieties. The occupancy of the major moiety refined to 62(1)%. The anisotropic displacement parameters of the carbon atoms involved in the disorder were restrained to be similar to those of their neighbors using DELU and SIMU commands from the Shelxtl program package. Default standard deviations were used. The ADPs of the two disordered nitrogen atoms were constrained to be identical. Equivalent bond distances in the disordered section were restrained to be the same in both moieties within a standard deviation of 0.02 Å. The second DEF molecule exhibits large and quite anisotropic displacement parameters. Attempts to refine the NEt₂ section of this ligand as disordered over two moieties, however, did not yield any improvements to the model and it seems that disorder of this molecule is dynamic in nature rather than a static disorder over several moieties. The sulfur bound hydrogen atoms were located in difference density Fourier maps but were ultimately placed at a fixed distance from the S atom with a U_{iso} value of 1.5 that of the respective sulfur atom. The H atoms were, however, allowed to

rotate around the C–S bond at a fixed C–S–H angle to best fit the experimental electron density. The lead complex (**2**) did not exhibit any disorder and required no use of constraints or restraints. Selected crystallographic results are summarized in Table 1, and full details of the crystallographic studies in cif format are included in the Supplementary Materials.

Table 1
Crystallographic data for **1**, **2** and **3**.

Compound	1	2	3
Chemical formula	C ₂₂ H ₄₆ Cu ₃ N ₁₀ O ₆ S ₃	C ₁₂ H ₁₈ N ₄ O ₄ Pb ₂ S ₂	C ₂₂ H ₂₈ EuN ₂ O ₈ S ₃
fw	833.49	760.80	696.64
Space group	<i>P</i> -1	<i>P</i> ₂ / <i>1</i> / <i>n</i>	<i>P</i> -1
<i>a</i> (Å)	9.757(1)	9.935(2)	10.150(1)
<i>b</i> (Å)	12.511(2)	7.442(2)	11.078(1)
<i>c</i> (Å)	14.862(2)	12.576(3)	13.878(2)
α (deg)	107.918(2)	90	107.373(2)
β (deg)	103.421(2)	105.568(2)	92.242(2)
γ (deg)	96.912(2)	90	115.042(1)
<i>V</i> (Å ³)	1642.7(3)	895.7(3)	1324.4(3)
<i>Z</i>	2	2	2
ρ calcd (g/cm ³)	1.685	2.821	1.747
GOF	1.022	1.130	1.056
<i>R</i> ₁ ^a [<i>I</i> > 2 σ (<i>I</i>)]	0.0326	0.0147	0.0342
<i>wR</i> ₂ ^b [<i>I</i> > 2 σ (<i>I</i>)]	0.0806	0.0366	0.0899

$$^a R_1 = \sum ||F_o| - F_c| / \sum (|F_o|)$$

$$^b wR_2 = (\sum [w(F_o^2 - F_c^2)] / \sum [w(F_o^2)])^{1/2}$$

3. Results and discussion

The solvothermal reaction of Cu(OAc)₂ · H₂O and H₄DMBD in ethylenediamine (en) at 100 °C for 2 days afforded yellow crystals of **1**. This reaction involved the reduction of Cu^{II} to Cu^I (presumably by the thiol units from DMBD as well as the amine function of en). Single-crystal X-ray analysis revealed that compound **1** (Cu₆(DMBD)₃(en)₄(Hen)₆) crystallizes in the space group *P*-1, with the asymmetric portion of the unit cell containing one and half DMBD⁴⁻ ions, three Cu(I) centers, two en molecules and three Hen⁺ ions. The three Cu(I) ions form a triangular Cu₃ cluster featuring significant Cu–Cu contacts (Cu–Cu distances: 2.647, 2.682 and 2.941 Å). The Cu₃ unit serves as a 3-connected node, and interacts with the DMBD⁴⁻ ions as a linear rod to form a distorted honeycomb coordination net parallel to the (11–1) plane (Fig. 1). Each of the three pairs of Cu(I) ions on the Cu₃ cluster is straddled by a thiolate S atom from the DMBD unit, with the six Cu–S distances ranging from 2.177 to 2.302 Å. In addition, Cu1 and Cu3 each are bonded to an amine group from an en molecule (Cu1–N, 2.062 Å, Cu3–N, 2.050 Å), while Cu2 is bonded to a carboxylate O atom that constitutes a chelation mode with the adjacent S atom from the same DMBD unit (Cu–O distance: 2.055 Å). Overall, all the S atoms are bonded to the Cu(I) centers, while only one of the three crystallographically independent carboxyl groups is coordinated (i.e., to Cu2). The other two carboxyl groups are deprotonated by the en molecules, which resulted in an extensive ionic hydrogen bond network that permeates the interstices of the coordination nets. The current system thus features a rich array of bonding types, including the

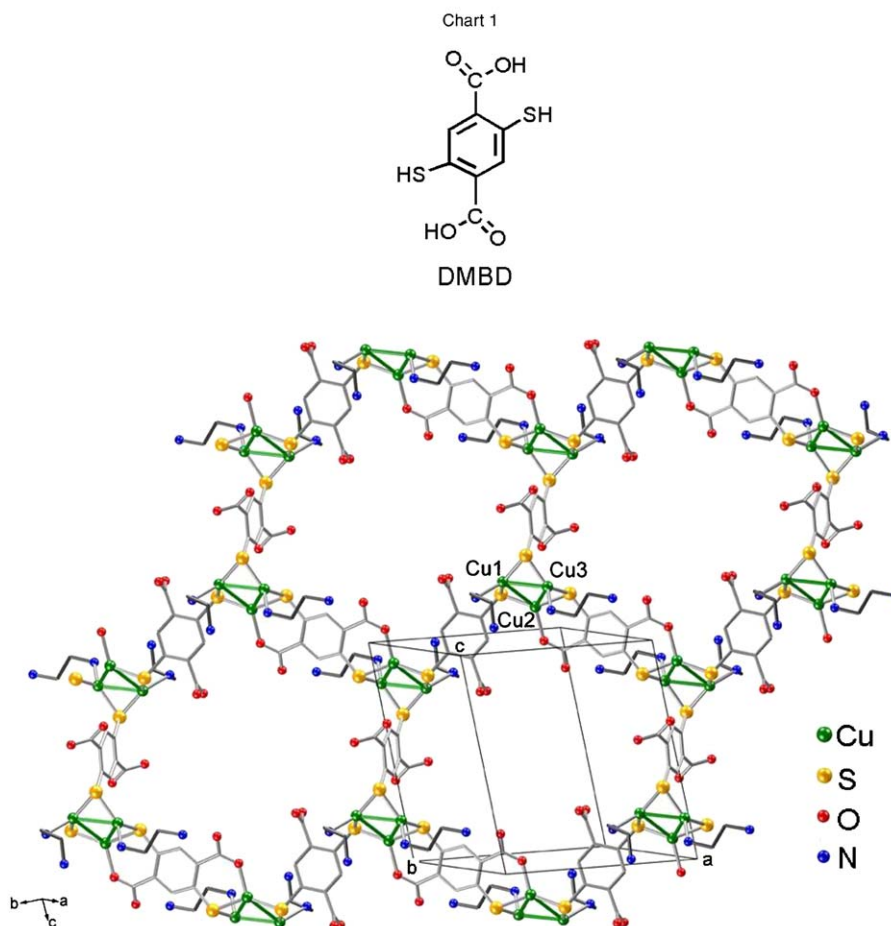


Fig. 1. An overview of the 2D coordination network of **1** (uncoordinating en species in the channels are omitted).

covalent-like thiolate–metal interaction, carboxylate–metal and amine–metal coordination, the ionic ammonium–carboxylate H bonding, and other weaker intermolecular interactions. We emphasize two major features of **1**: (1) the fully bonded S atoms (to Cu^+ ions) and the partially coordinated carboxyl groups, which is consistent with their respective soft–hard natures and the consequently different affinity to the soft $\text{Cu}(\text{I})$ center; (2) the Cu_3 cluster, as a commonly reported motif in isolated polynuclear thiolatocopper(I) species [11], has now been integrated into a 2D thiolate network here.

By comparison, all the carboxyl and thiol groups are engaged by the slightly harder $\text{Pb}(\text{II})$ ions in $\text{Pb}_2(\text{DMBD})(\text{en})_2$ (**2**). Specifically, the asymmetric portion of the unit cell contains one

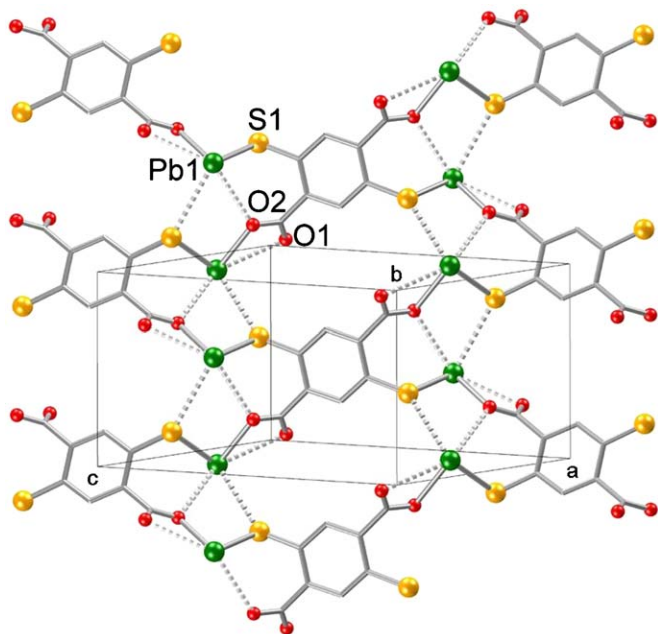


Fig. 2. The coordination environment of the $\text{Pb}(\text{II})$ centers and the resultant 2D net of **2**. Dotted lines represent elongated (secondary) contacts.

$\text{Pb}(\text{II})$ ion, and half of a DMBD^{4-} ion and one en molecule: each Pb center is bound by an en molecule (in chelation mode, $\text{Pb}-\text{N}$ distances: 2.497, 2.571 Å), a carboxylate group (in chelation mode, $\text{Pb}-\text{O}$ distances: 2.559, 2.884 Å), and a thiolate S atom from another DMBD^{4-} ion ($\text{Pb}-\text{S}$ distances: 2.679 Å). With the $\text{Pb}(\text{II})$ ion thus serving as a linear rod between the DMBD units, and each DMBD^{4-} ion as a four connected node, a distorted parallelogram net can be derived from the resultant 2D coordination network (Fig. 2). Notice that, unlike the 2D infinite Cu –thiolate network in **1**, the thiolate–metal interactions in **2** are broken into isolated domains by the coordination units of the O or N donors, which might weaken the electronic communication throughout the network. Other notable features include helices formed along the *b* axis by the thiolate–carboxylate– $\text{Pb}(\text{II})$ units (Figure S1). However, the chirality of **2** vanishes in each layer because the right-handed (R) and left-handed (L) enantiomers appear in pairs.

By contrast, the even harder Eu^{3+} ion bonds exclusively to the carboxyl groups of H_4DMBD , leading to a 3D framework in $\text{Eu}_2(\text{H}_2\text{DMBD})_3(\text{DEF})_4$ (**3**) with free-standing thiol groups. Complex **3** (space group: *P*-1) features an unusual $\text{Eu}_2(\text{COO})_6$ cluster (Fig. 3a) with an $\text{Eu}-\text{Eu}$ distance of 4.033 Å as its secondary building block. In the centrosymmetric $\text{Eu}_2(\text{COO})_6$ cluster, the roles of the carboxylate groups divide into three types: one chelates a single Eu^{3+} ion ($\text{Eu}-\text{O}$ distances: 2.475, 2.525 Å), another bridges the two metal ions ($\text{Eu}-\text{O}$ distances: 2.395, 2.425 Å), and the last simultaneously chelates to one Eu^{3+} ion ($\text{Eu}-\text{O}$ distances: 2.441, 2.632 Å) and bridges across to the other Eu^{3+} ion using one of the O atoms ($\text{Eu}-\text{O}$ distance: 2.405 Å). Overall, each Eu ion is bonded to six O atoms from the carboxylate groups, together with two O atoms from the two DEF molecules ($\text{Eu}-\text{O}$ distance: 2.433 Å). With the $\text{Eu}_2(\text{COO})_6$ unit as a 6-connected node and the H_2DMBD unit as a linear rod, the resultant 3D coordination net features a distorted α -Po topology. No interpenetration occurs, and the void space is taken up by the DEF molecules. Preliminary effort to remove the DEF molecules by evacuation under heat caused the collapse of the host network. Further exploration is ongoing to establish conditions for achieving a stable porous net, in order to make the free-standing thiol units accessible to guest species such as metal ions and other species reactive to the $-\text{SH}$ group (e.g., H_2O_2 , Br_2).

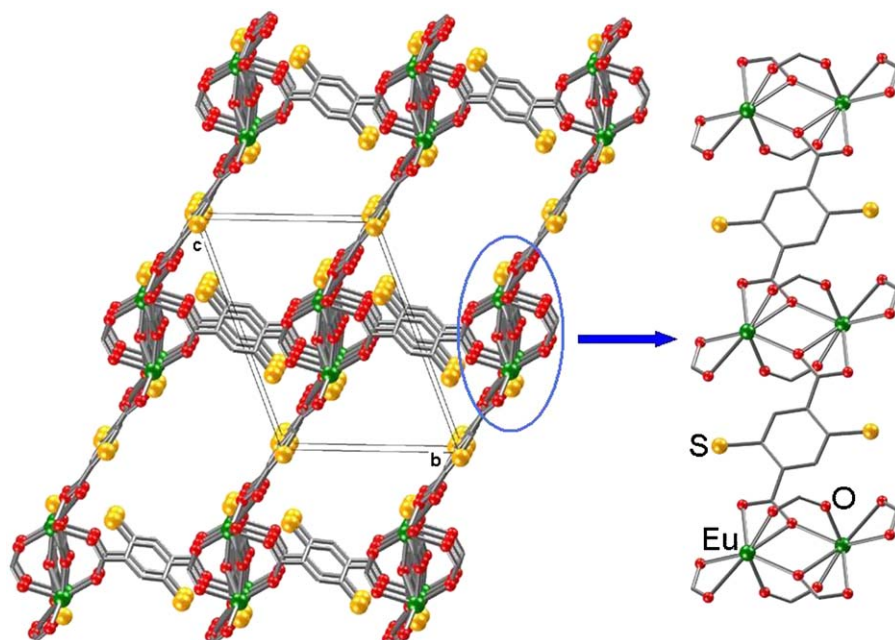


Fig. 3. View of the 3D coordination net of **3** along the *a* axis (left, the DEF molecules are omitted), and the connection of the $\text{Eu}_2(\text{COO})_6$ units along the *a* axis (right).

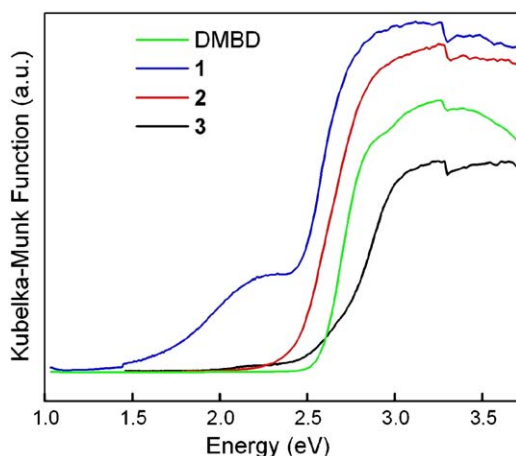


Fig. 4. Room temperature optical absorption spectra for solid samples of H₄DMBD and **1–3**.

To probe the impact of metal–thiolate interaction on solid state electronic properties, we here present the preliminary results from the diffuse reflectance spectra of **1**, **2**, **3** and the ligand H₄DMBD (Fig. 4). By fitting the steepest slope on the absorption edge (wherein the Kubelka–Munk function is proportional to the absorption coefficient α) vs. the photon energy and extrapolating to $\alpha = 0$, the band gaps (E_g) of 2.43, 2.48 and 2.58 eV were obtained for **2**, **3** and H₄DMBD, respectively. As shown in Fig. 4, the similarity in the absorption features of **2**, **3** and H₄DMBD suggests domination of the ligand-centered excitation, although the Pb–S interactions in **2** might have helped red shift its absorption edge relative to **3** and H₄DMBD. The Cu₃S₃ cluster-based system of **1**, however, features an additional, relatively broad absorption at substantially lower energy (about 1.61 eV). This new feature could be associated with the splitting of the frontier orbitals on the Cu₃ cluster due to the Cu...Cu interactions [12], which lowers the energy of the cluster-centered LUMOs and consequently the energy of the electronic transitions between the ligand and the metal centers. Taken together, the preliminary electronic property study here fits well with the electroactivity generally observed of the metal–thiolate interactions, even though further electronic structure studies are needed to reveal more details regarding the mechanisms of the optical transitions observed in these solid state systems.

4. Conclusion

In summary, the increasing hardness in Cu(I), Pb(II) and Eu(III) correlates well with the decreasing dominance of the soft mercapto groups in the coordination motifs of **1**, **2** and **3**. The preliminary synthetic exercises here also demonstrate the potentially rich structural and functional possibilities offered by the carboxyl–mercapto combination in constructing coordination networks. Specifically, the readily crystallizable Cu(I) and Pb(II)–thiolate networks in **1** and **2** point to the facilitating role of the carboxylate groups in the crystallization process, a role that might also be relevant in crystallizing a wider range of metal–thiolate networks; the free-standing thiol groups on the metal carboxylate framework of **3**, on the other hand, suggest an interesting avenue to functionalizing the commonly studied metal carboxylate networks, in that the thiol groups could potentially be involved in post-crystallization processes such as taking up heavy metal ions or covalent cross-linking. In addition, the anionic host net of **1** provides the opportunity to ion-exchange with the Hen⁺ guest

cations in order to modify the electronic property of the host net or provide for potential solid state ionic conductivity.

Supplementary materials

Additional figures of the crystal structure of **2**. X-ray powder diffraction patterns for **1**, **2** and **3**. Full crystallographic data in CIF format for **1**, **2** and **3**. Thermogravimetric analysis (TGA) plots for **1** and **3**. Crystallographic data (excluding structure factors) for the structures reported in this paper have been deposited with the Cambridge Crystallographic Data Centre as supplementary publication no. CCDC 713331–713333. Copies of the data can be obtained free of charge on application to CCDC, 12 Union Road, Cambridge CB2 1EZ, UK (fax: +44 1223 336 033; e-mail: deposit@ccdc.cam.ac.uk).

Acknowledgments

This work is supported by City University of Hong Kong (Project no. 7002119) and the Research Grants Council of HKSAR [Project 9050198 (N_CityU 118/06)]. The diffractometer was funded by NSF Grant 0087210, by Ohio Board of Regents Grant CAP-491, and by Youngstown State University.

Appendix A. Supplementary material

Supplementary data associated with this article can be found in the online version at doi:10.1016/j.jssc.2009.04.024.

References

- [1] Selected reviews: K.T. Holman; A.M. Pivovarov; J.A. Swift; M.D. Ward, *Acc. Chem. Res.* 34 (2001) 107–118; J.D. Wuest, *Chem. Commun.* (2005) 5830–5837; S.J. Dalgarno, P.K. Thallapally, L.J. Barbour, J.L. Atwood, *Chem. Soc. Rev.* 36 (2007) 236–245; S.R. Batten, R. Robson, *Angew. Chem. Int. Ed.* 37 (1998) 1461–1494; O.R. Evans, W. Lin, *Acc. Chem. Res.* 35 (2002) 511–522; L. Carlucci, G. Ciani, D.M. Proserpio, *Coord. Chem. Rev.* 246 (2003) 247–289; S. Kitagawa, R. Kitaura, S.-i. Noro, *Angew. Chem. Int. Ed.* 43 (2004) 2334–2375; S. Lee, A.B. Mallik, Z. Xu, E.B. Lobkovsky, L. Tran, *Acc. Chem. Res.* 38 (2005) 251–261; D. Bradshaw, J.B. Claridge, E.J. Cussen, T.J. Prior, M.J. Rosseinsky, *Acc. Chem. Res.* 38 (2005) 273–282; N.W. Ockwig, O. Delgado-Friedrichs, M. O’Keeffe, O.M. Yaghi, *Acc. Chem. Res.* 38 (2005) 176–182; K.S. Suslick, P. Bhyrappa, J.H. Chou, M.E. Kosal, S. Nakagaki, D.W. Smitherly, S.R. Wilson, *Acc. Chem. Res.* 38 (2005) 283–291; T.C.W. Mak, L. Zhao, *Chem. Asian J.* 2 (2007) 456–467; D. Maspocho, D. Ruiz-Molina, J. Veciana, *Chem. Soc. Rev.* 36 (2007) 770–818; D. Tanaka, S. Kitagawa, *Chem. Mater.* 20 (2008) 922–931; G. Férey, *Chem. Soc. Rev.* 37 (2008) 191–214.
- [2] C.J. Kepert, M.J. Rosseinsky, *Chem. Commun.* (1998) 31–32; H. Li, M. Eddaoudi, M. O’Keeffe, O.M. Yaghi, *Nature* 402 (1999) 276–279; H.K. Chae, D.Y. Siberio-Perez, J. Kim, Y.B. Go, M. Eddaoudi, A.J. Matzger, M. O’Keeffe, O.M. Yaghi, *Nature* 427 (2004) 523–527; X. Zhao, B. Xiao, A.J. Fletcher, K.M. Thomas, D. Bradshaw, M.J. Rosseinsky, *Science* 306 (2004) 1012–1015; G. Férey, C. Mellot-Draznieks, C. Serre, F. Millange, J. Dutour, S. Surble, I. Margiolaki, *Science* 309 (2005) 2040–2042; X. Lin, A.J. Blake, C. Wilson, X.Z. Sun, N.R. Champness, M.W. George, P. Hubberstey, R. Mokaya, M. Schröder, *J. Am. Chem. Soc.* 128 (2006) 10745–10753; J.Y. Lee, D.H. Olson, L. Pan, T.J. Emge, J. Li, *Adv. Funct. Mater.* 17 (2007) 1255–1262; S. Ma, D. Sun, M. Ambrogio, J.A. Fillinger, S. Parkin, H.-C. Zhou, *J. Am. Chem. Soc.* 129 (2007) 1858–1859; F. Nouar, J.F. Eubank, T. Bousquet, L. Wojtas, M.J. Zaworotko, M. Eddaoudi, *J. Am. Chem. Soc.* 130 (2008) 1833–1835;

- B. Chen, L. Wang, F. Zapata, G. Qian, E.B. Lobkovsky, *J. Am. Chem. Soc.* 130 (2008) 6718–6719.
- [3] G.N. Schrauzer, H. Prakash, *Inorg. Chem.* 14 (1975) 1200–1204;
P. Feng, X. Bu, N. Zheng, *Acc. Chem. Res.* 38 (2005) 293–303;
C.-M. Che, S.-H. Li, S.S.-Y. Chui, V.A.L. Roy, K.-H. Low, *Chem. Eur. J.* 14 (2008) 2965–2975;
J. Li, W. Bi, W. Ki, X. Huang, S. Reddy, *J. Am. Chem. Soc.* 129 (2007) 14140–14141;
X. Huang, J. Li, *J. Am. Chem. Soc.* 129 (2007) 3157–3162;
Z. Zhang, J. Zhang, T. Wu, X. Bu, P. Feng, *J. Am. Chem. Soc.* 130 (2008) 15238–15239;
D.B. Mitzi, M. Yuan, W. Liu, A.J. Kellock, S.J. Chey, V. Deline, A.G. Schrott, *Adv. Mater.* 20 (2008) 3657–3662;
D.B. Mitzi, L.L. Kosbar, C.E. Murray, M. Copel, A. Afzali, *Nature* 428 (2004) 299–303;
M.G. Kanatzidis, *Acc. Chem. Res.* 38 (2005) 359–368;
H. Li, A. Laine, M. O'Keeffe, O.M. Yaghi, *Science* 283 (1999) 1145–1147;
J.B. Parise, *Science* 251 (1991) 293–294.
- [4] W. Su, M. Hong, J. Weng, R. Cao, S. Lu, *Angew. Chem. Int. Ed.* 39 (2000) 2911–2914;
Y. Zhao, M. Hong, Y. Liang, R. Cao, J. Weng, S. Lu, W. Li, *Chem. Commun.* (2001) 1020–1021;
Z. Chen, L.R. Sutton, D. Moran, A. Hirsch, W. Thiel, P.v.R. Schleyer, *J. Org. Chem.* 68 (2003) 8808–8814;
J. Beck, Y. Ben-Amer, *Z. Anorg. Allg. Chem.* 633 (2007) 435–439;
D.L. Turner, T.P. Vaid, P.W. Stephens, K.H. Stone, A.G. DiPasquale, A.L. Rheingold, *J. Am. Chem. Soc.* 130 (2008) 14–15;
X.-Y. Tang, H.-X. Li, J.-X. Chen, Z.-G. Ren, J.-P. Lang, *Coord. Chem. Rev.* 252 (2008) 2026–2049;
J. Beck, Y. Ben-Amer, *Z. Anorg. Allg. Chem.* 634 (2008) 1522–1526.
- [5] E. Neofotistou, C.D. Malliakas, P.N. Trikalitis, *Inorg. Chem.* 46 (2007) 8487–8489.
- [6] L. Field, P.R. Engelhardt, *J. Org. Chem.* 35 (1970) 3647–3655;
L. Vial, R.F. Ludlow, J. Leclaire, R. Perez-Fernandez, S. Otto, *J. Am. Chem. Soc.* 128 (2006) 10253–10257.
- [7] J.S. Seo, D. Whang, H. Lee, S.I. Jun, J. Oh, Y.J. Jeon, K. Kim, *Nature* 404 (2000) 982–986;
Z. Xu, S. Lee, Y.-H. Kiang, A.B. Mallik, N. Tsomaia, K.T. Mueller, *Adv. Mater.* 13 (2001) 637–641;
- P. Brunet, E. Demers, T. Maris, G.D. Enright, J.D. Wuest, *Angew. Chem. Int. Ed.* 42 (2003) 5303–5306;
C.-D. Wu, A. Hu, L. Zhang, W. Lin, *J. Am. Chem. Soc.* 127 (2005) 8940–8941;
K.K. Tanabe, Z. Wang, S.M. Cohen, *J. Am. Chem. Soc.* 130 (2008) 8508–8517;
Z. Wang, S.M. Cohen, *Angew. Chem. Int. Ed.* 47 (2008) 4699–4702.
- [8] X.-P. Zhou, Z. Xu, M. Zeller, A.D. Hunter, S.S.-Y. Chui, C.-M. Che, *Inorg. Chem.* 47 (2008) 7459–7461.
- [9] Selected examples of thioether-based coordination networks: M.B. Inoue, M. Inoue, M.A. Bruck, Q. Fernando, *Chem. Commun.* (1992) 515–516;
X. Gan, M. Munakata, T. Kuroda-Sowa, M. Maekawa, *Bull. Chem. Soc. Jpn.* 67 (1994) 3009–3011;
J.C. Zhong, Y. Misaki, M. Munakata, T. Kuroda-Sowa, M. Maekawa, Y. Suenaga, H. Konaka, *Inorg. Chem.* 40 (2001) 7096;
Y. Suenaga, H. Konaka, K. Kitamura, T. Kuroda-Sowa, M. Maekawa, M. Munakata, *Inorg. Chim. Acta* 351 (2003) 379–384;
Y.-T. Fu, V.M. Lynch, R.J. Lagow, *Chem. Commun.* (2004) 1068–1069;
L. Do, S.R. Halper, S.M. Cohen, *Chem. Commun.* (2004) 2662–2663;
K. Li, Z. Xu, H. Xu, P.J. Carroll, J.C. Fettingner, *Inorg. Chem.* 45 (2006) 1032–1037;
Z. Xu, *Coord. Chem. Rev.* 250 (2006) 2745–2757;
G. Huang, H. Xu, X.-P. Zhou, Z. Xu, K. Li, M. Zeller, A.D. Hunter, *Cryst. Growth Des.* 7 (2007) 2542–2547;
G. Huang, C.-K. Tsang, Z. Xu, K. Li, M. Zeller, A.D. Hunter, S.S.-Y. Chui, C.-M. Che, *Cryst. Growth Des.* 9 (2009) 1444–1451.
- [10] R.G. Parr, R.G. Pearson, *J. Am. Chem. Soc.* 105 (1983) 7512–7516.
- [11] G. Henkel, B. Krebs, *Chem. Rev.* 104 (2004) 801–824;
J.R. Nicholson, I.L. Abrahams, W. Clegg, C.D. Garner, *Inorg. Chem.* 24 (1985) 1092–1096;
M. Baumgartner, H. Schmalle, *J. Solid State Chem.* 107 (1993) 63–75;
M. Baumgartner, H. Schmalle, E. Dubler, *Inorg. Chim. Acta* 208 (1993) 135–143;
C.P. Rao, J.R. Dorfman, R.H. Holm, *Inorg. Chem.* 25 (1986) 428–439;
G. Dance, L.J. Fitzpatrick, M.L. Scudder, *J. Chem. Soc. Chem. Commun.* (1983) 546–548;
A. Müller, F.W. Baumann, H. Bögge, K. Schmitz, *Z. Anorg. Allg. Chem.* 521 (1985) 89–96.
- [12] P.C. Ford, E. Cariati, J. Bourassa, *Chem. Rev.* 99 (1999) 3625–3647;
V.W.-W. Yam, K.K.-W. Lo, *Chem. Soc. Rev.* 28 (1999) 323–334.